Fault Diagnosis for a Wind Turbine Generator Bearing via Sparse Representation and Shift-Invariant K-SVD

Boyuan Yang, *Student Member, IEEE*, Ruonan Liu, *Student Member, IEEE*, and Xuefeng Chen, *Member, IEEE*

Abstract—It is always a primary challenge in fault diagnosis of a wind turbine generator to extract fault character information under strong noise and nonstationary condition. As a novel signal processing method, sparse representation shows excellent performance in time–frequency analysis and feature extraction. However, its result is directly influenced by dictionary, whose atoms should be as similar with signal's inner structure as possible. Due to the variability of operation environment and physical structure in industrial systems, the patterns of impulse signals are changing over time, which makes creating a proper dictionary even harder. To solve the problem, a novel data-driven fault diagnosis method based on sparse representation and shift-invariant dictionary learning is proposed. The impulse signals at different locations with the same characteristic can be represented by only one atom through shift operation. Then, the shift-invariant dictionary is generated by taking all the possible shifts of a few short atoms and, consequently, is more applicable to represent long signals that in the same pattern appear periodically. Based on the learnt shift-invariant dictionary, the coefficients obtained can be sparser, with the extracted impulse signal being closer to the real signal. Finally, the time–frequency representation of the impulse component is obtained with consideration of both the Wigner–Ville distribution of every atom and the corresponding sparse coefficient. The excellent performance of different fault diagnoses in a fault simulator and a wind turbine proves the effectiveness and robustness of the proposed method. Meanwhile, the comparison with the state-of-the-art method is illustrated, which highlights the superiority of the proposed method.

Index Terms—Fault diagnosis, periodical impulse vibration extraction, redundant union of dictionaries, shift-invariant dictionary learning, sparse time–frequency representation, wind turbine generator.

I. INTRODUCTION

WIND energy has experienced a remarkable expansion in recent years to improve the serious environment problems and deal with the shortage of fossil fuels [1], [2]. However, wind turbines are usually operated in extreme and harsh environment, which generate rapid changes on temperature, air pressure, wind shear, wind speed, and total load. These variations make wind turbines undergo constantly changing global and local dynamics and loads and, therefore, lead to relatively higher failure rates [3], [4]. The failures of a wind turbine not only cause stability problems, but also result in high cost for repairing and maintenance, especially for those large and remotely located wind turbines [5]. It is reported that operation and maintenance (O&M) costs account for up to 30% of the energy generation costs, while 66% of O&M costs are caused by unexpected failures [6]. Therefore, many researchers have conducted various research works to condition monitoring and fault diagnosis technology of wind turbines.

A generator is one of the most important components in a wind turbine, which is easy to malfunction because of severe operation environment and wide-range fluctuation of loads [7]. The contributions of offshore wind turbine components to the total O&M costs and downtime are given in Fig. 1. It can be seen that generator failure is one of the three most common failures. The failures of a blade, a generator, and a gearbox contribute together for over 76% of the costs and over 87% of the downtime. The cost caused by the generator is nearly one-fifth of the total cost, and the downtime is nearly one-third. Therefore, an effective fault diagnosis method for a wind turbine generator is essential for wind turbine maintenance decisions.

The failure modes in electric motors can be classified as electrical faults and mechanical faults [8]. The electrical faults mainly include: 1) stator faults resulting in the opening or shorting of one or more of a stator phase winding; and 2) broken rotor bar or cracked rotor. The mechanical faults mainly include bearing failure, rotor unbalance, rotor misalignment, and bowed rotor. These faults can result in the change of vibration signal, current signal, torque, temperature, and so on. Mechanical faults such as bearing and shaft faults constitute a significant portion of all faults in wind turbine generators [9], [10]. The reported failure surveys have shown that bearing problems account for between 21% and 95% of all failures in electrical machines [11].
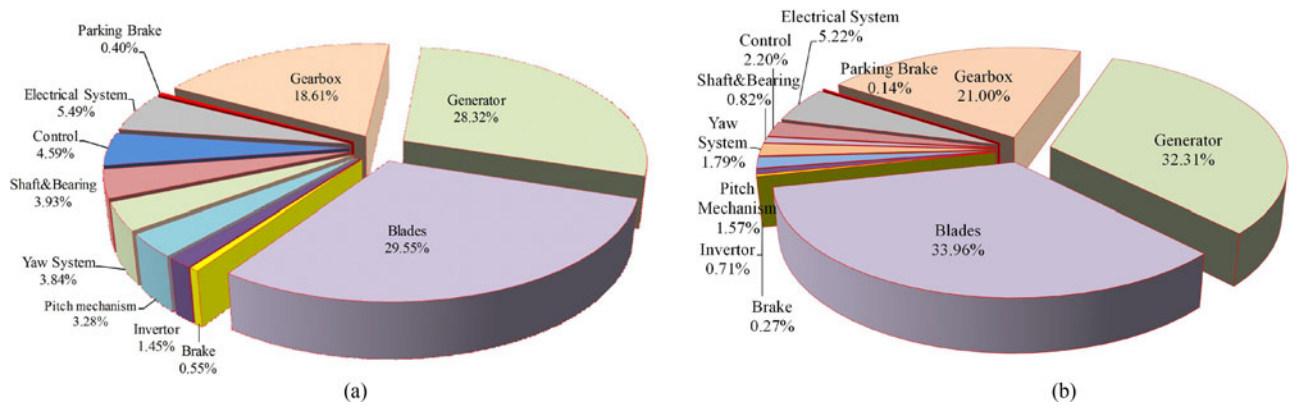
Fig. 1. Relative contribution of the components to the costs and downtime of wind turbine. (a) Distribution of costs. (b) Distribution of downtime.

The percentage failure by components in induction machines is typically the following: about 40% failures are related to bearings, 38% to the stator, 10% to the rotor, and 12% to others [12], [13]. As a result, the fault diagnosis of generators has received an intense amount of research interest during the last 30 years [14].

For the purpose of reducing maintenance costs and extracting representative features from the complex nonstationary noisy signal, numerous signal processing approaches have been developed for fault diagnosis of electric generators used in wind turbines, such as statistical analysis, Fourier transform [15], wavelet transform [16], [17], Hilbert–Huang transform [18], and empirical mode decomposition [19], [20].

Different from traditional diagnosis methods, sparse representation [21] aims to find sparsest or nearly sparsest representations of signal that capture higher level features in the data over redundant dictionaries. The main idea of sparse representation theory is to concentrate the energy of feature information into a few elements and provide a feasible way to identify multiple feature information simultaneously by projecting different fault signals into different sparse representation spaces. Due to the powerful ability of extracting features, sparse representation methods have been rapidly developed for fault diagnosis, including matching pursuit (MP) [22], basis pursuit denoising [23], and manifold sparse reconstruction [24]. Effective as they are, a lot of prior knowledge is needed to apply them in industrial systems. The representation effectiveness is directly influenced by the selection of dictionary, which is difficult in fault diagnosis of a generator due to the changeable operation environment, complex components, and nonstationary condition. Dictionary learning is an effective data-driven way to construct an empirically learned dictionary for sparse representation, in which the generating atoms come from the underlying empirical data, rather than from some theoretical models. The most commonly used dictionary learning method is K-SVD [25], which builds the dictionary by alternating a sparse approximation of the training signals on the current dictionary and the optimization of the dictionary according to the computed decomposition. However, when dealing with a long signal, the dictionary learning method needs to split the signal into small frames, and even the same frames with different phases will result in different atoms. As a result, the learnt dictionary will be huge with a lot of redundant information. Due to the characteristics of mechanical signals such as strong periodicity, variability, and the phase problem, it can be useful to learn a shift-invariant dictionary.

Therefore, based on the characteristics of mechanical signals, a sparse time–frequency representation method combined with a shift-invariant dictionary learning technique is proposed for fault diagnosis of wind turbine generator bearings, which overcomes the limitations of the traditional sparse representation and dictionary learning method. All impulsive features at different locations with the same characteristics can be represented by just one basis function by the proposed method, with no need to split long signals into small frames. Therefore, the learnt dictionary is smaller and more applicable for vibration signals in industrial systems with a faster convergence speed compared with K-SVD.

This paper is organized as follows. Section II describes the physical background and the mechanical vibration model of a wind turbine generator. In Section III, the proposed shift-invariant dictionary learning algorithm and the sparse time–frequency representation technique are illustrated in detail and verified by a synthetic signal. In Section IV, an experiment performed on a fault simulator and a field test are performed to illustrate the effectiveness of the proposed method. Conclusion and future work of the research are presented in Section V.

II. MECHANICAL VIBRATION MODEL OF A GENERATOR

Vibration data are recognized as the best parameter in a wind turbine (WT) for incipient fault diagnosis during the operation [26], because it can reflect operational condition and faults properties rapidly, accurately and comprehensively. There are three mainly components in the generator vibration signal, with strong coupling effect.

A. Harmonic Component

Limited to manufacturing precision, the rotor in the generator is neither completely symmetrical and axisymmetric on the physical structure nor completely coaxial with the bearings. Therefore, when the rotor rotates, these unbalances and misalignments will cause vibration that is made up of harmonics

with frequencies of the rotation frequency and its multiplications. The vibration can be described as

$$s_h(t) = \sum_{m=0}^{M} A_m \cos(2\pi m f_r t + \phi_m), \qquad m \in N^+ \quad (1)$$

where A_m and ϕ_m are amplitude and phase of the m times rotation frequency component, respectively, and f_r is the rotor rotation frequency.

B. Periodic Impulse Component

In the generator with a faulty bearing, impulse vibration will be generated when a ball passes through the defect, which can be represented as

$$s_i(t) = \sum_k h(t - T_0 - kT) \quad (2)$$

where T_0 is the initial phase. $T = 1/f_{\text{fault}}$ is the time interval between two impulse. $h(t)$ is a single impulse that varies from different operation conditions. The fault characteristic frequency f_{fault} is set to be f_i, f_o, f_b, and f_c, respectively, when the fault occurs on inner race, outer race, ball, and cage:

$$\begin{aligned}
f_i &= 0.5 N_B f_r \left(1 + \frac{D_b \cos\theta}{D_c}\right) \\
f_o &= 0.5 N_B f_r \left(1 - \frac{D_b \cos\theta}{D_c}\right) \\
f_b &= 0.5 f_r \left(\frac{D_c}{D_b}\right) \left[1 - \left(\frac{D_b \cos\theta}{D_c}\right)^2\right] \\
f_c &= 0.5 f_r \left(1 - \frac{D_b \cos\theta}{D_c}\right)
\end{aligned} \quad (3)$$

where N_B is the number of balls in the bearing, D_b is the ball diameter, D_c is the pitch diameter, and θ is the ball contact angle.

C. Mixed Signal

These vibration components are often distorted by relatively strong noises, which may arise from sensor imperfection, poor running environment or communication errors, and so on. Therefore, the vibration caused by the generator is a combination of three components: harmonic vibration, periodic impulse vibration, and noise. The observed vibration signal of a generator in the wind turbine often can be described as

$$s(t) = s_h(t) + s_i(t) + n(t). \quad (4)$$

It is worth noting that the power of the generator is provided by natural wind, and the rotation frequency of the generator changes with wind speed. As a result, the parameters f_{fault} and T in (2) change constantly.

III. PROPOSED ALGORITHM

Based on the physical background and sparse representation framework, a novel fault diagnosis method is proposed for fault diagnosis of a wind turbine generator bearing, which mainly includes three steps: harmonic components separation, shift-invariant K-SVD dictionary learning, and sparse time–frequency representation.

A. Sparse Representation Model

The main idea of sparse representation is to replace the basis function sets with overcompleted redundant function sets, which are called the overcompleted dictionary, and then trace the parameterized functions matched with the signal structure feature. As a result, signal can be represented as a linear combination of few vectors, which are called atoms in the dictionary.

Given an overcompleted set $D = g_k; k = 1, 2, ..., K$. The K elements in D constitute the unit vectors, which span the whole Hilbert space $H = \mathbb{R}^N$. If $K \geq N$, the set D is called the overcompleted dictionary and the element in D is called the atom. For any signal $f \in H$, m atoms are selected adaptively to m-term approximate the signal $s(t)$:

$$s = \sum_{\gamma \in I_m} \alpha_\gamma g_\gamma \quad (5)$$

where I_m is the set of parameter γ, and g_γ is the atom determined by γ.

In sparse representation theory, the components in dictionary D is nonorthogonal and overcompleted. Therefore, selecting the sparsest representation of signal $s(t)$ from D is equivalent to the following optimization problem:

$$\min \|\alpha\|_0 \quad \text{s.t.} \quad s = D\alpha \quad (6)$$

where α is the sparse coefficients, and norm $\|\alpha\|_0$ is defined as the number of nonzero coefficients in a coefficient vector.

When $s(t)$ is noisy, then the optimization problem is transformed as

$$\min \|\alpha\|_0 \quad \text{s.t.} \quad s - D\alpha < \varepsilon. \quad (7)$$

Various greedy algorithms and convex optimization techniques could be employed to solve (6) and (7), such as MP [27], orthogonal matching pursuit (OMP) [28], stagewise OMP [29], and basis pursuit [30].

B. Harmonic Component Separation

Harmonic components spread all over the vibration signal and can cause modulation effect on the impact component and, consequently, influence the result of impulsive feature extraction, which is a fundamental transient phenomenon that always modeled as dynamic response of abnormal operations when the generator develops local malfunction [31]. Therefore, the first stage of the proposed algorithm is separating the harmonic components from the vibration signal.

The vibration signal in (4), by introducing a dictionary D_1, can be expressed as

$$s(t) = s_h(t) + s_i(t) + n(t) = D_1 \alpha_1 + s_i(t) + n(t) \quad (8)$$

where α_1 is the coefficient vector of the harmonic component under the combined dictionary.

The aim of sparse representing harmonic components is to find their frequencies. Therefore, frequency dictionary, which

---

Harmonic Separation Algorithm

Input: Signal s

       Threshold value ε

Initialize: $D_0 = 0$, $k = 0$, $R^0 s = s$

Procedure:

1. Create Fourier dictionary D

2. Compute $\langle R^k s, g_n \rangle$, $g_n \in D \backslash D_k$

   Find $\left| \langle R^k s, g_{n_{k+1}} \rangle \right| \geq \alpha \sup_j \left| \langle R^k s, g_j \rangle \right|$, $0 < \alpha \leq 1$

3. If $\left| \langle R^k s, g_{n_{k+1}} \rangle \right| < \varepsilon$, then stop

4. Reorder the dictionary D, by applying the permutation $k+1 \leftrightarrow n_{k+1}$

5. Compute $\{b_n^k\}_{n=1}^k$, such that $g_{k+1} = \sum_{n=1}^k b_n^k g_n + \gamma_k$

   and $\langle \gamma_k, g_n \rangle = 0$, $n = 1, \cdots, k$

6. Set $a_{k+1}^{k+1} = \alpha_k = \|\gamma_k\|^{-2} \langle R^k s, g_{k+1} \rangle$

   $a_n^{k+1} = a_n^k - \alpha_k b_n^k$, $n = 1, \cdots, k$

   and update the model

   $s_{k+1} = \sum_{n=1}^{k+1} a_n^{k+1} g_n$ $R^{k+1} s = s - s_{k+1}$ $D_{k+1} = D_k \bigcup \{g_{k+1}\}$

7. Set $k \leftarrow k+1$ and repeat 2-7.

Output: $s_r(t) = R^k s$

Fig. 2. Harmonic separation algorithm.

takes frequency as a parameter variable, can sparsely represent the harmonic components and keep the impact components. The Fourier dictionary is a typical frequency dictionary constructed by a collection of trigonometric functions. Therefore, the sub-dictionary for harmonic components D_1 is set to be the Fourier dictionary. The atom in the Fourier dictionary can be represented by a trigonometric function with a parameter $\gamma = (f, \upsilon)$, where f is the frequency parameter and $\upsilon \in 0, 1$ is the phase parameter. When $\upsilon = 0$, the atom is a cosine function, and when $\upsilon = 1$, it is a sine function:

$$g_s(f, 0) = \cos(2\pi f t), \quad g_s(f, 1) = \sin(2\pi f t). \quad (9)$$

Then, the Fourier dictionary is used to match the vibration signal, and the optimization problem of separating harmonic components can be described as

$$\underset{\alpha_1}{\arg\min} \|\alpha_1\|_0 \quad \text{s.t.} \quad s - D_1 \alpha_1 < \epsilon. \quad (10)$$

The optimization problem is solved by the OMP, which is profoundly described in Fig. 2. After α_1 is obtained, the harmonic component can be estimated as $\hat{s}_h = D_1 \alpha_1$. Therefore, the combination signal of impact components and noise can be obtained as $s_r(t) = R^k s$. $R^k s$ is the residual signal after k iterations.

C. Shift-Invariant K-SVD Dictionary Learning

It is easy to construct a suitable dictionary to sparsely represent harmonic components because of their fixed structure. However, due to the various failure modes in electric machines, the internal structures of impact components vary from different failures and make it difficult to select a proper dictionary to fit the impact signals. Therefore, it can be useful to learn a dictionary from signals.

After separating harmonic components, the dictionary learning problem under the combination of impact components and noise $s(t)$ can be expressed as the computation of a dictionary that minimizes the approximation error under a hard sparsity constraint:

$$\min_{\|\alpha\|_0 \leq L} \sum_l \|s_l - D\alpha_l\|_2^2 \quad (11)$$

where L is the maximum number of atoms, and l is the number of samples.

However, traditional dictionary learning methods such as K-SVD [25] are sensitive to the position and phase. That is, even two same signals with different position or phase will result in two different atoms. And learning from vibration signals directly will result in time-localized atoms with arbitrary position, and each shift of pattern will lead to another atom. At the same time, with the wide distribution of rotating components in generators, the vibration signals are strong cyclical and shift invariant. It would be more efficient and effective to learn a shift-invariant dictionary. Therefore, shift-invariant K-SVD [32], which is an extension of K-SVD, is used for dictionary learning to separate the impact component.

In shift-invariant K-SVD, the learning is performed on one long signal, instead of splitting the signal into frames in K-SVD, and the dictionary D_2 is built by shifting a family M of patterns m: $M = (m_k)_{1 \leq k \leq K}$. All impulsive features at different locations with the same characteristics can be represented by just one basis function, which is called the pattern. Therefore, the learning problem is turned into learning the set of patterns and can be defined by the new objective function:

$$\min_{\|\alpha\|_0 \leq L} \left\| s - \sum_k \sum_\tau \alpha_{k,\tau} m_k(t - \tau) \right\|_2^2$$

$$= \min_{\|\alpha\|_0 \leq L} \left\| s - \sum_k \sum_\tau \alpha_{k,\tau} T_\tau m_k \right\|_2^2 \quad (12)$$

where T_τ is the shift operator that takes a pattern m and returns an atom that is null everywhere except for a copy of m that starts at instant τ. Therefore, the dictionary D_2 can be defined as $D_2 = (T_\tau m_k)_k, \tau$.

Shift-invariant K-SVD is composed of alternation of sparse decomposition stage and dictionary update stage, which follows the iterative strategy as the K-SVD algorithm. The main difference between them is that shift-invariant K-SVD relies on the instants where they are not null instead of the value of the amplitude coefficients. And it deals with the dictionary learning problem by updating each pattern m_k successively and the amplitude coefficients c_k, τ, accordingly before updating the next pattern.

The purpose of the sparse decomposition stage is to find the closest sparse approximation of a signal. There are many suboptimal algorithms that can be used to solve the problem, and the MP algorithm [33] is applied in this paper because it performs well in dealing with highly coherent and large dictionaries.

In the dictionary update stage, the patterns are updated to minimize the error. For a given pattern m_κ, define the signal

---

Shift-invariant K-SVD Algorithm

Input: Signal s; sparsity L; length of atom l; number of atom K.

Initialize: M_0: m_{0_k} is selected randomly from s with the length of l;
$\quad\quad\quad i = 0$.

Procedure:

1. Compute sparse coefficient α by MP in shift-invariant case:

$$\widehat{\alpha_i} = \arg\min_{\alpha} \left\| s - \sum\sum \alpha_{k,\tau} T_\tau m_{i_k} \right\|_2^2 \quad \text{s.t. } \|\alpha\|_0 \leq L$$

2. Update M_i and α_i according to (16) and (17);
3. $i \leftarrow i + 1$ until the change of $\left\| s - \sum_k \sum_\tau \alpha_{k,\tau} T_\tau m_{i_k} \right\|_2^2$ is small enough.

Output: M, $\alpha_{k,\tau}$.

Fig. 3. Shift-invariant K-SVD algorithm used for dictionary learning.

without the contributions of the other patterns m_k, $k \neq \kappa$, as

$$\hat{s}_\kappa = r + \sum_\tau \alpha_{\kappa,\tau} T_\tau m_\kappa. \tag{13}$$

Then, the best update pattern m_κ^{opt} can be given by

$$(m_\kappa^{\text{opt}}, \alpha_\kappa^{\text{opt}}) = \underset{\|m\|_2 = 1}{\arg\min} \left\| \hat{s}_\kappa - \sum_{\tau \in \sigma_\tau} \alpha_\tau T_\tau m \right\|_2^2. \tag{14}$$

As the shift operators T_τ are unitary, the objective function can be defined as

$$\left\| \hat{s}_\kappa - \sum_{\tau \in \sigma_\tau} \alpha_\tau T_\tau m \right\|_2^2 = \sum_{\tau \in \sigma_\tau} \| T_\tau^* \hat{s}_\tau - \alpha_\tau m \|_2^2 + cst, \quad \forall m \tag{15}$$

where T_τ^* is the adjoint of T_τ. It extracts a patch with the same length as a pattern from a signal and begins at τ. Then

$$m_\tau \leftarrow \underset{\|m\|_2 = 1}{\arg\min} \sum_{\tau \in \sigma_\tau} \langle m, T_\tau^* \hat{s}_\kappa \rangle^2 \tag{16}$$

$$(\alpha_{\kappa,\tau})_{\tau \in \sigma_\kappa} \leftarrow \arg\min \left\| \hat{s}_\kappa - \sum_{\tau \in \sigma_\tau} \alpha_\tau T_\tau m \right\|_2^2. \tag{17}$$

More specifically, the shift-variant K-SVD algorithm is illustrated in Fig. 3. The computational cost is mainly concentrated in procedure 1. In this step, the fast algorithm described in [33] is applied, whose computing complexity of this step is order of $O(l \log l)$. For a signal s with length N, if the algorithm is converged after i iterations, there are $ikNl \log l$ times of multiplication operations that are required to run the shift-invariant K-SVD algorithm.

The extracted signal can be reconstructed by

$$\hat{s}_i(t) = \sum_k \sum_\tau \alpha_{k,\tau} m_k(t - \tau). \tag{18}$$

D. Sparse Time–Frequency Representation

According to the step of shift-invariant K-SVD dictionary learning, M and $\alpha_{k,\tau}$ can be obtained. Each atom in the dictionary has its time–frequency characteristics, which can be represented by many time–frequency distribution methods, such as the short-time Fourier transform, the Wigner–Ville distribution (WVD), and the wavelet transform. In this paper, the WVD is

employed due to its advantage of high time–frequency resolution. The WVD of the kth atom can be defined as

$$W_{\text{atom}(k)}(t, f) = \sum_{-\infty}^{\infty} m_{(k)}\left(t + \frac{\tau}{2}\right) m_{(k)}^*\left(t - \frac{\tau}{2}\right) e^{-j2\pi ft}. \tag{19}$$

After n iterations, the WVD of all atoms can be obtained. Then, the sparse time–frequency representation of the reconstructed impulse signal $\hat{s}_i$ can be implemented by integrating the WVD of the atoms with nonzero coefficient and corresponding sparse coefficients:

$$\text{STF}_s(t, f) = \sum_k \sum_\tau \alpha_{k,\tau} W_{\text{atom}(k)}(t - \tau). \tag{20}$$

E. Verification by a Synthetic Signal

To verify the performance of the proposed method, a synthetic signal is constructed. According to the mechanical vibration model in Section II, the simulation signal consists of harmonic component, periodic impact component, and Gaussian white noise:

$$
\begin{aligned}
x(t) &= x_1(t) + x_2(t) + n(t) \\
&= 0.3\sin(2\pi f_r t + \pi/3) \\
&\quad + \sum_k h(t - T_0 - kT) + n(t)
\end{aligned} \tag{21}
$$

where $x_1(t)$ is the harmonic component and $x_2(t)$ is the periodic impact component. $h(t)$ is defined as

$$h(t) = \exp\left[\left(-\frac{\xi}{\sqrt{1 - 2\xi^2}} 2\pi f_n t\right) \sin(2\pi f_n t)\right] \quad t \geq 0 \tag{22}$$

where f_r is set to be 33 Hz. f_n is 500 Hz, T_0 is 0.05 s, T is 0.1 s, and $t \in [0, 10]$s. That is, the signal contains 100 periodic impact components used for learning the atom. The signal-to-noise ratio is set to be -11.141 dB. The waveforms of a synthetic signal are shown in Fig. 4.

Then, the simulated signal is processed by the proposed method. The sampling frequency should be at least twice as much as f_n. In this simulation, the sampling frequency is set to be 6400 Hz. The learnt shift-invariant atom is shown in Fig. 5. The size of the learnt atom should be bigger than the duration time of an oscillation and smaller than the time interval between two impacts. The reconstructed harmonic and impact components are displayed in Fig. 6. And the sparse time–frequency distribution of impact signal is shown in Fig. 7.

It can be seen that the learnt atom is basically the same as the simulation impact signal. In addition, the periodic impulse component can be observed obviously with the oscillation frequency of 500 Hz. Therefore, the proposed method shows excellent performance under strong noise disturbance.

IV. APPLICATIONS AND DISCUSSIONS

To verify the effectiveness of the proposed method, two experiments are performed. The first one is performed on a simulator test rig, and a field test is performed as the second experiment.
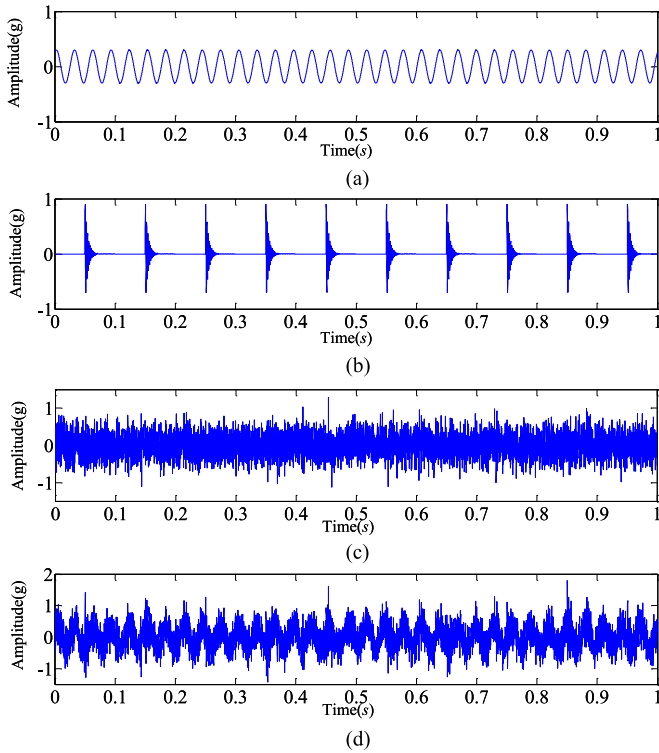
Fig. 4. Simulation signal. (a) Harmonic component. (b) Impact component. (c) Noise. (d) Synthetic signal.
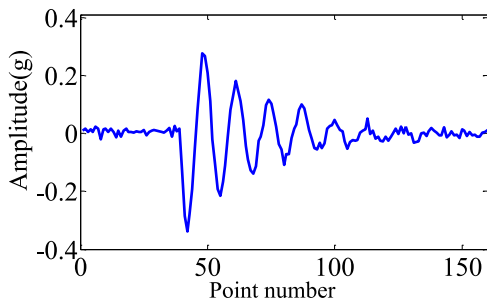
Fig. 5. Shift-invariant atom learnt by the proposed method.
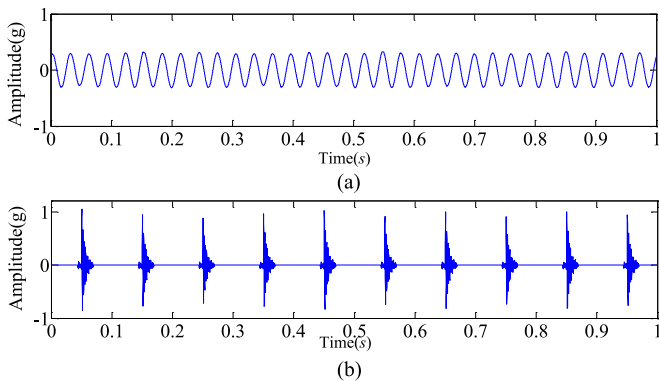
Fig. 6. Reconstructed signal of (a) the harmonic component and (b) the impact component.
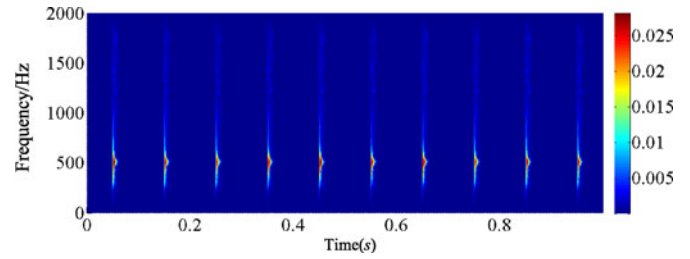
Fig. 7. Sparse time–frequency distribution of the impact component.
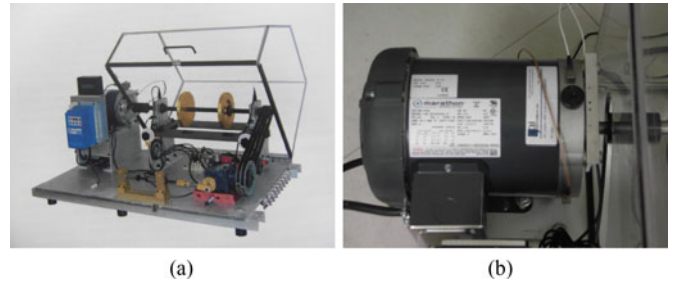
Fig. 8. SQI test rig for an electric machine simulator. (a) Overall view of the SQI test rig. (b) Enlarged view on the position of sensors.
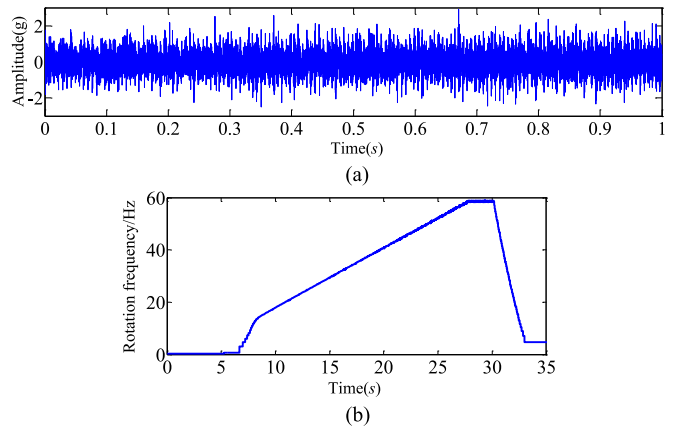
Fig. 9. (a) Analyzed signal. (b) Rotation frequency.

The results of the two experiments and the comparison with other method are reported in detail.

A. Fault Simulation Test

The first experiment was conducted on an SQI electric machine fault simulator, as shown in Fig. 8. SKF 6203 bearing is used in this experiment. The fault characteristic frequency of the outer race is 4.932 Hz when the rotation frequency of the output shaft is 1 Hz, which can be calculated via (3). A simulated peeling-off fault is conducted on the bearing outer race. The vibration signals are acquired by an accelerometer with the sampling frequency of 12 800 Hz. The rotation speed ranges from 0 to 3600 r/min. One segment of the vibration signals and the change of the rotation frequency are displayed in Fig. 9.
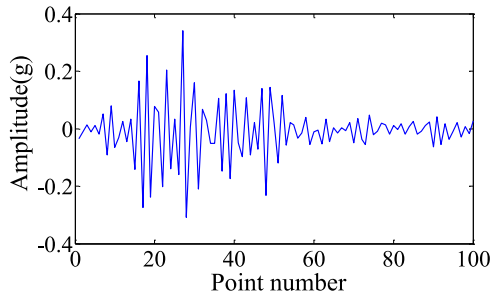
Fig. 10.   Waveforms of the learnt atom.
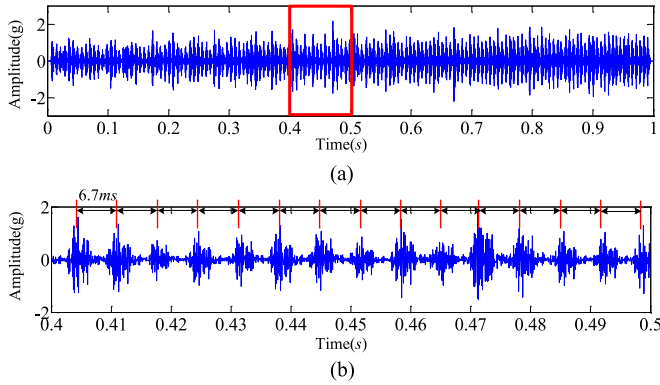
Fig. 11.   Results obtained by the proposed method. (a) Extracted impact component and (b) its local enlarged detail. The period of impulsive signals indicates that there is a local fault in the outer race.
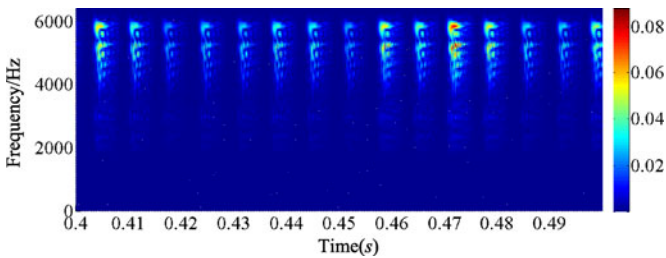
Fig. 12.   Sparse time–frequency distribution of the extracted impulse signal.

Then, the proposed method is applied to analyze the vibration signal from 15 to 16 s, which is in the speed increment. Fig. 10 graphically illustrates the learnt shift-invariant atom. The resulting impulse component through the proposed method and a zoom-in view with a length of 0.1 s are depicted in Fig. 11. Furthermore, the sparse time–frequency distribution of the subcomponent is illustrated in Fig. 12. It can be seen clearly that the impulsive components appear periodically. In this experiment, the diameter of the defect is about 1.5 mm, and the depth is 0.5 mm. The detail of the defect is shown in Fig. 13.

In this segment of signal, the rotation frequency ranges from 30.1 to 30.4 Hz. Based on the fault characteristic frequency of the outer race and the rotation frequency range, the corresponding fault characteristic frequency of the bearing outer race can be calculated by rotation frequency $\times 4.932$ Hz, which ranges

Fig. 13.   Defect on the outer race of the experimental bearing.

from 148.453 to 149.933 Hz. Therefore, the impulse interval can be obtained as the reciprocal of fault characteristic frequency, which is between 6.670 and 6.736 ms, and agree with the extracted signal and its time–frequency distribution in Figs. 10 and 11. But the frequency band is in wide range, which indicates that multiple natural frequencies are motivated when a roller passing through the peeling off of the outer race and impulse occurs. It can be inferred that the impact energy components in the range of 4000–6000 Hz in Fig. 12 are caused by the resonance oscillations of bearing components when the bearing is passing the defect. The center frequency is related to the first-order radial inherent vibration of the vibration system [34].

For comparison, the same vibration signal is analyzed by spectrum kurtosis (SK) and K-SVD methods. The results of SK are shown in Fig. 14. There are also some impulse components can be observed in the SK-filtered signal. However, they are not as obvious and clear as the result of the proposed method, and the periodicity is also not significant. And the existence of cross-term interference also influences the time–frequency distribution. Besides, due to the dictionary learning technique and the properties of being data driven, the proposed method does not rely on the prior knowledge. On the contrary, the frequency band range should be determined first when using SK. Therefore, the obtained vibration of the impulse signal concentrates on about 5600 Hz.

The results of K-SVD after 20 iterations are shown in Figs. 14 and 15. The length of atom is set to be 100 points, which is kept the same with the proposed method. The number of atoms in the dictionary is set to be 256. Fig. 15 shows two atoms of the 256 learnt atoms. Fig. 16 shows the denoised signal and its local enlarged detail from 0.4 to 0.5 s. From the results, it can hardly be found some very unclear periodic impulse components. Therefore, compared with the proposed method, K-SVD is inefficient to diagnose the fault. For the vibration signals in this experiment, the running time of the K-SVD method is 17.5575 s, while the running time of the proposed method is 0.5543 s on a corei3-3320 @ 3.3-GHz computer. Therefore, the proposed method also shows advantages of computational cost and practicability in industrial applications.

To further evaluate the effectiveness of the proposed method, a health electric machine was tested on the same SQI test bed,
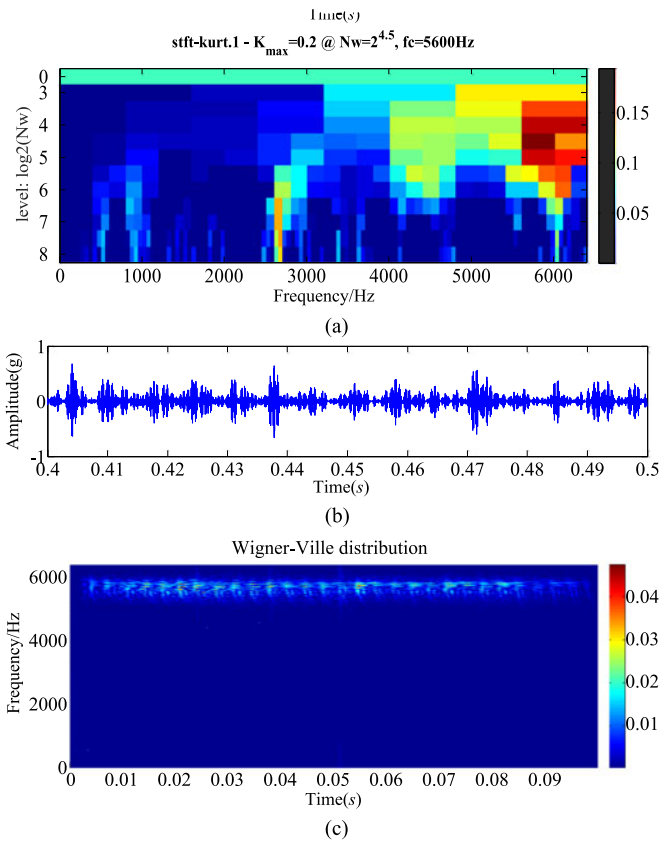
Fig. 14. Results obtained by SK. (a) Fast kurtogram of the vibration signals. (b) Filtered signal according to the optimal filter. (c) WVD of the filtered signal.
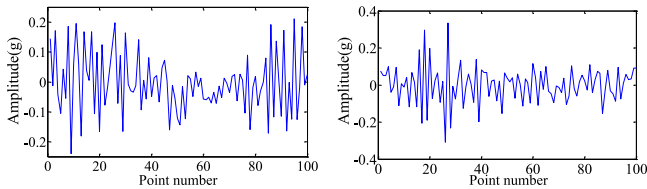
Fig. 15. Waveforms of two learnt atoms.
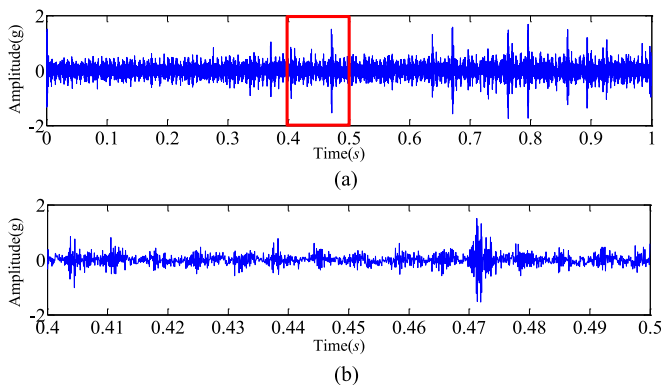
Fig. 16. Results obtained by K-SVD. (a) Denosied signal and (b) its local enlarged detail. It can hardly found the periodic impulse components.
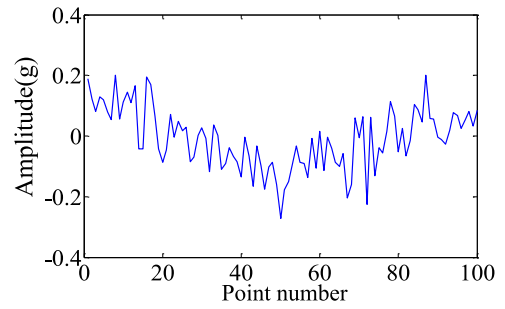
Fig. 17. Learnt atom.
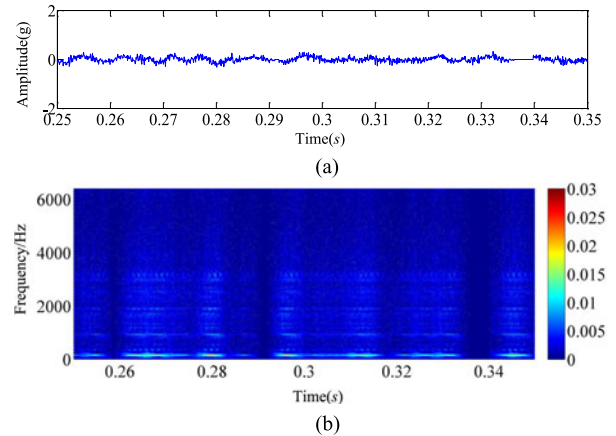
Fig. 18. Results obtained by the proposed method. (a) Extracted impact component and (b) its sparse time–frequency distribution.

and the collected signal is analyzed. The parameters are both kept the same. The learnt atom is illustrated in Fig. 17, and little oscillation and feature information can be found.

The reconstructed impact signal and its sparse time–frequency distribution are shown in Fig. 18(a) and (b). It can be seen that there are only some low-frequency vibration with a small amplitude in the reconstructed signal and the sparse time–frequency distribution. Therefore, the proposed method has the ability to distinguish healthy and faulty cases.

B. Wind Field Test

During one inspection in a wind field, the vibration data collected by accelerate sensors from the generator of an abnormal wind turbine are over the standard. The sensor is located at the front of a generator bearing with the type of SKF 6326C3, as shown in Fig. 19. The sampling frequency is 25 600 Hz. One segment of 5-s vibration signal with decreasing rotation speed is displayed in Fig. 20. It can be seen that the rotation speed changes quickly, and there is no significant feature information for fault diagnosis.

Then, the proposed method is applied to extract an impulse vibration signal in this field test. The shift-invariant atom in the dictionary learnt by the proposed method is shown in Fig. 21.

The extracted impulse signal and its local enlarged detail are shown in Fig. 22, with the rotating frequency ranging from

Fig. 19. Generator in the wind field. (a) Overall view of the generator. (b) Position of the sensor.
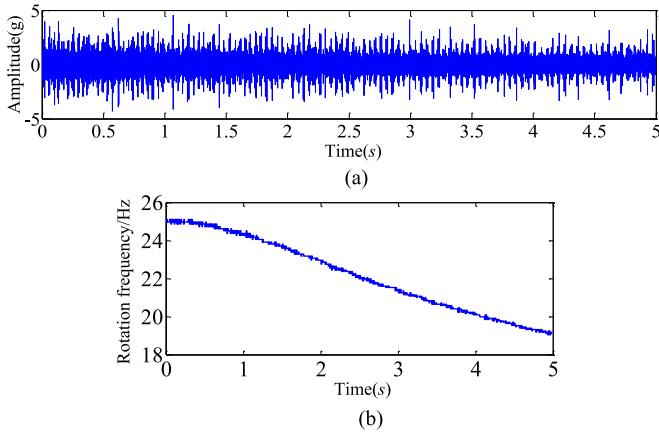
Fig. 20. (a) Analyzed signal. (b) Rotation frequency.
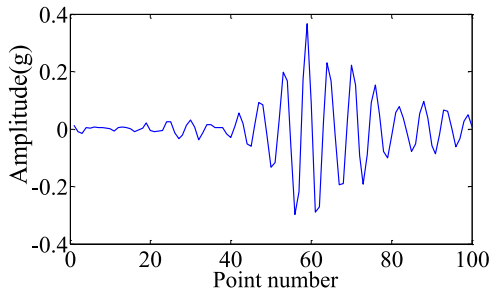
Fig. 21. Learnt atom.
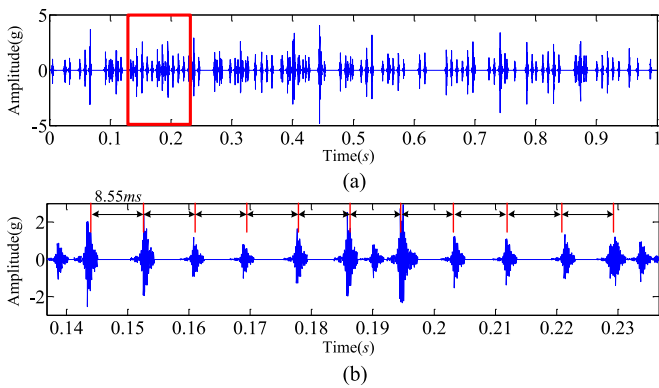
Fig. 22. Results obtained by the proposed method. (a) Extracted impact component and (b) its local enlarged detail. The period of impulsive components matches with the inner race fault.
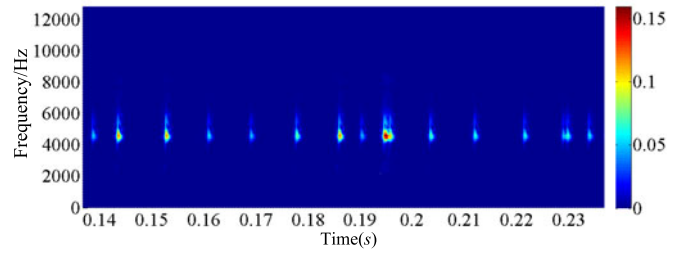
Fig. 23. Sparse time–frequency distribution of the extracted impulse component.

TABLE I
IMPULSE INTERVAL OF THE BEARING

Positions	Characteristic frequency	Range of impulse interval/ms
Outer race	[74.93, 75.31]	[13.28, 13.35]
Inner race	[116.43, 117.01]	[8.55, 8.59]
Rolling element	[105.13, 105.66]	[9.46, 9.51]
Cage	[9.37, 9.41]	[106.22, 106.76]
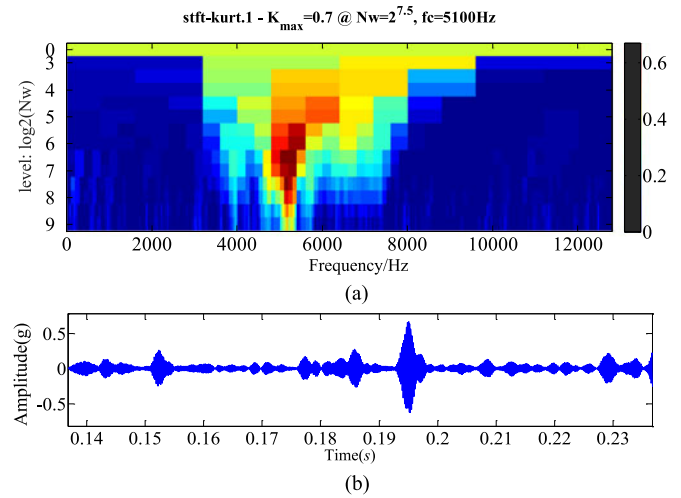
Fig. 24. Results obtained by SK. (a) Fast kurtogram of the vibration signals. (b) Filtered signal according to the optimal filter.

23.92 to 24.04 Hz. Its time–frequency distribution is shown in Fig. 23. Table I lists the impulse intervals of the bearing that are calculated according to (3).

We found the clear periodic impulse signals in Fig. 22 with the interval of 8.55 ms, which agree with the theoretical value of the inner race fault. Therefore, it can be concluded that there is a localized fault that exists on the bearing inner race. Then, a comprehensive inspection is performed on the wind turbine generator, and a local damage is found on the inner race of the front bearing.

The same vibration signal is processed by SK for comparison. The results are displayed in Fig. 24.

It can be seen that the characteristic pattern of the fault is not significant. In addition, although there are some impulse components being extracted, the weak impulse are submerged
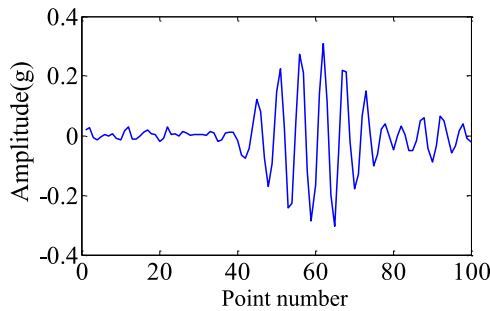
Fig. 25.　Learnt atom.
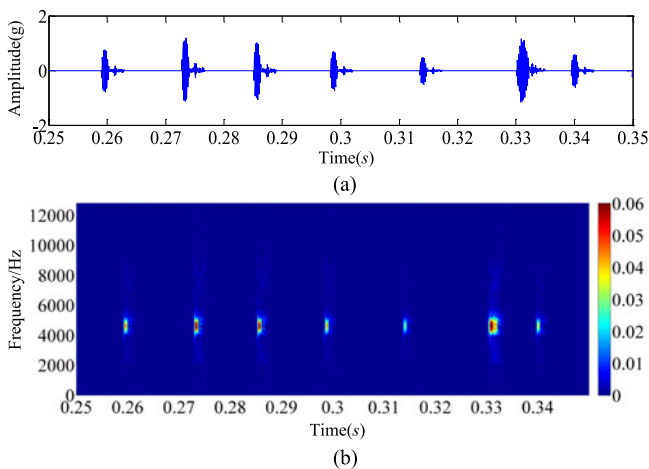
Fig. 26.　Results obtained by the proposed method. (a) Extracted impact component and (b) its sparse time–frequency distribution.

by the strong noise and no periodic components can be found. Therefore, the SK technique is not as efficient as the proposed method for impulse vibration signals extraction, especially under nonstationary and strong noise conditions.

To further illustrate the robustness of the proposed method, another signal of the same wind turbine is analyzed as well, whose rotation frequency ranges from 15.5 to 16 Hz. The parameters of the approach are kept to be the same. The learnt shift-invariant atom is shown in Fig. 25. The extracted impact component and its sparse time–frequency distribution are shown in Fig. 26.

The fault characteristic frequency of inner race ranges from 75.44 to 77.88 Hz, and the corresponding impact interval ranges from 12.84 to 13.26 ms, which are matching with Fig. 26. Therefore, as long as the impulse interval time is longer than the oscillation time of the impact component, this method can work well, and the choice of the rotation frequency will not impact the quality of the results.

V. CONCLUSION

The periodic impulsive feature is always modeled as vibration response of abnormal operations in a faulty generator. However, the characteristic of impulsive component varies from different generator systems. Therefore, in this paper, a data-driven

fault diagnosis method for a wind turbine generator bearing is proposed based on the idea of sparse representation and shift-invariant dictionary learning to extract different impulsive components from vibration signal. Compared with traditional sparse representation methods, it overcomes the dependence of prior knowledge and the selection of proper dictionary, while extracting the impulse component more effectively. Moreover, the proposed method can represent the impulses at different locations with the same characteristic by just one basis function, which is very suitable for analyzing the fault signal with periodic impulses. The verification results of both the fault simulation test and the actual wind field test demonstrate that the proposed method can learn shift-invariant atoms adaptively and extract the valuable impulse components precisely from different generator systems. The comparison with the recognized method also proves the effectiveness and robustness of the proposed method for fault diagnosis of wind turbine generator bearings under nonstationary and strong noise conditions. Future work will pay more attention to composite fault detection and the improvement of parameter self-adaption, such as the threshold value, the atom number, and the size of the learnt atom.

REFERENCES

[1] F. Blaabjerg and K. Ma, "Future on power electronics for wind turbine systems," *IEEE J. Emerg. Sel. Topics Power Electron.*, vol. 1, no. 3, pp. 139–152, Sep. 2013.

[2] S. Yu, T. Fernando, and H. H.-C. Iu, "Realization of state-estimation-based DFIG wind turbine control design in hybrid power systems using stochastic filtering approaches," *IEEE Trans. Ind. Informat.*, vol. 12, no. 3, pp. 1084–1092, Jun. 2016.

[3] W. Qiao and D. Lu, "A survey on wind turbine condition monitoring and fault diagnosis‡part i: Components and subsystems," *IEEE Trans. Ind. Electron.*, vol. 62, no. 10, pp. 6536–6545, Oct. 2015.

[4] H. D. M. de Azevedo, A. M. Araújo, and N. Bouchonneau, "A review of wind turbine bearing condition monitoring: State of the art and challenges," *Renew. Sustain. Energy Rev.*, vol. 56, pp. 368–379, 2016.

[5] F. Blaabjerg and K. Ma, "Future on power electronics for wind turbine systems," *IEEE J. Emerg. Sel. Topics Power Electron.*, vol. 1, no. 3, pp. 139–152, Sep. 2013.

[6] P. Asmus and M. Seitzler, "The wind energy operation & maintenance report," Wind Energy Update, London, U.K., 2010. [Online]. Available: http://social.windenergyupdate.com/

[7] J. Chen, J. Pan, Z. Li, Y. Zi, and X. Chen, "Generator bearing fault diagnosis for wind turbine via empirical wavelet transform using measured vibration signals," *Renew. Energy*, vol. 89, pp. 80–92, 2016.

[8] J. Seshadrinath, B. Singh, and B. Panigrahi, "Vibration analysis based interturn fault diagnosis in induction machines," *IEEE Trans. Ind. Informat.*, vol. 10, no. 1, pp. 340–350, Feb. 2014.

[9] M. Paolone *et al.*, "Models of wind-turbine main shaft bearings for the development of specific lightning protection systems," in *Proc. IEEE Lausanne Power Tech*, 2007, pp. 783–789.

[10] X. Gong and W. Qiao, "Bearing fault diagnosis for direct-drive wind turbines via current-demodulated signals," *IEEE Trans. Ind. Electron.*, vol. 60, no. 8, pp. 3419–3428, Aug. 2013.

[11] P. Tavner, "Review of condition monitoring of rotating electrical machines," *IET Electr. Power Appl.*, vol. 2, no. 4, pp. 215–247, 2008.

[12] R. Bell, C. Heising, P. O'donnell, C. Singh, and S. Wells, "Report of large motor reliability survey of industrial and commercial installations: Part II," *IEEE Trans. Ind. Appl.*, vol. IA-21, no. 4, pp. 865–872, Jul. 1985.

[13] A. H. Bonett and G. C. Soukup, "Cause and analysis of stator and rotor failures in three-phase squirrel-cage induction motor," *IEEE Trans. Ind. Appl.*, vol. 28, no. 4, pp. 921–937, Jul./Aug. 1992.

[14] H. Henao *et al.*, "Trends in fault diagnosis for electrical machines: A review of diagnostic techniques," *IEEE Ind. Electron. Mag.*, vol. 8, no. 2, pp. 31–42, Jun. 2014.

[15] R. Klein, D. Ingman, and S. Braun, "Non-stationary signals: Phase-energy approach‡theory and simulations," *Mech. Syst. Signal Process.*, vol. 15, no. 6, pp. 1061–1089, 2001.

[16] R. Yan, R. X. Gao, and X. Chen, "Wavelets for fault diagnosis of rotary machines: A review with applications," *Signal Process.*, vol. 96, pp. 1–15, 2014.

[17] H. Keskes and A. Braham, "Recursive undecimated wavelet packet transform and DAG SVM for induction motor diagnosis," *IEEE Trans. Ind. Informat.*, vol. 11, no. 5, pp. 1059–1066, Oct. 2015.

[18] N. E. Huang, *Hilbert-Huang Transform and its Applications*, vol. 16. Singapore: World Scientific, 2014.

[19] N. E. Huang *et al.*, "The empirical mode decomposition and the hilbert spectrum for nonlinear and non-stationary time series analysis," *Proc. Roy. Soc. London A, Math., Phys. Eng. Sci.*, vol. 454, pp. 903–995, 1998.

[20] Y. Lei, J. Lin, Z. He, and M. J. Zuo, "A review on empirical mode decomposition in fault diagnosis of rotating machinery," *Mech. Syst. Signal Process.*, vol. 35, no. 1, pp. 108–126, 2013.

[21] W. Jiang, Z. Zhang, F. Li, L. Zhang, M. Zhao, and X. Jin, "Joint label consistent dictionary learning and adaptive label prediction for semisupervised machine fault classification," *IEEE Trans. Ind. Informat.*, vol. 12, no. 1, pp. 248–256, Feb. 2016.

[22] R. Liu, B. Yang, X. Zhang, S. Wang, and X. Chen, "Time-frequency atoms-driven support vector machine method for bearings incipient fault diagnosis," *Mech. Syst. Signal Process.*, vol. 75, pp. 345–370, 2016.

[23] H. Yang, J. Mathew, and L. Ma, "Fault diagnosis of rolling element bearings using basis pursuit," *Mech. Syst. Signal Process.*, vol. 19, no. 2, pp. 341–356, 2005.

[24] X. Ding and Q. He, "Time–frequency manifold sparse reconstruction: A novel method for bearing fault feature extraction," *Mech. Syst. Signal Process.*, vol. 80, pp. 392–413, 2016.

[25] A. Michal, E. Michael, and B. Alfred, "K-SVD: Design of dictionaries for sparse representation," in *Proc. Signal Process. Adaptive Sparse Struct. Represent. Workshop*, 2005, vol. 5, pp. 9–12.

[26] W. Li, S. Zhang, and S. Rakheja, "Feature denoising and nearest–farthest distance preserving projection for machine fault diagnosis," *IEEE Trans. Ind. Informat.*, vol. 12, no. 1, pp. 393–404, Feb. 2016.

[27] S. G. Mallat and Z. Zhang, "Matching pursuits with time-frequency dictionaries," *IEEE Trans. Signal Process.*, vol. 41, no. 12, pp. 3397–3415, Dec. 1993.

[28] J. A. Tropp and A. C. Gilbert, "Signal recovery from random measurements via orthogonal matching pursuit," *IEEE Trans. Inf. Theory*, vol. 53, no. 12, pp. 4655–4666, Dec. 2007.

[29] D. L. Donoho, Y. Tsaig, I. Drori, and J.-L. Starck, "Sparse solution of underdetermined systems of linear equations by stagewise orthogonal matching pursuit," *IEEE Trans. Inf. Theory*, vol. 58, no. 2, pp. 1094–1121, Feb. 2012.

[30] S. S. Chen, D. L. Donoho, and M. A. Saunders, "Atomic decomposition by basis pursuit," *SIAM Rev.*, vol. 43, no. 1, pp. 129–159, 2001.

[31] V. C. Leite *et al.*, "Detection of localized bearing faults in induction machines by spectral kurtosis and envelope analysis of stator current," *IEEE Trans. Ind. Electron.*, vol. 62, no. 3, pp. 1855–1865, Mar. 2015.

[32] B. Mailhé, S. Lesage, R. Gribonval, F. Bimbot, and P. Vandergheynst, "Shift-invariant dictionary learning for sparse representations: Extending K-SVD," in *Proc. 16th Eur. Signal Process. Conf.*, 2008, pp. 1–5.

[33] S. Krstulovic and R. Gribonval, "MPTK: Matching pursuit made tractable," in *Proc. IEEE Int. Conf. Acoust. Speech Signal Process.*, 2006, vol. 3, p. III.

[34] R. B. Randall and J. Antoni, "Rolling element bearing diagnostics‡a tutorial," *Mech. Syst. Signal Process.*, vol. 25, no. 2, pp. 485–520, 2011.

Boyuan Yang (S'16) received the B.S. degree in mechanical engineering (in Qian Xuesen Experimental Class) in 2013 from Xi'an Jiaotong University, Xi'an, China, where he is currently working toward the Ph.D. degree in mechanical engineering.

His current interests include wind turbine fault diagnostics, signal sparse representation and time–frequency representation, data-driven prognostics, and health management.

Ruonan Liu (S'15) received the B.S. degree in mechanical engineering from Xi'an Jiaotong University, Xi'an, China in 2013, where she is currently working toward the Ph.D. degree in mechanical engineering.

Her current research focuses on machine learning, deep learning, and sparse signal representation for mechanical signal processing, diagnosis, and prognosis for industrial systems.

Xuefeng Chen (M'12) received the Ph.D. degree in mechanical engineering from Xi'an Jiaotong University, Xi'an, China, 2004.

He is a Professor of mechanical engineering with Xi'an Jiaotong University. His current research interests include finite-element method, machinery condition monitoring, and prognostics.

Dr. Chen received the National Excellent Doctoral Dissertation of China in 2007, the Second Awards of Technology Invention of China in 2009, and the National Science Fund for Distinguished Young Scholars in 2012.